

Deuteron fluctuations and proton-deuteron correlations from the STAR experiment at $\sqrt{s_{NN}} = 7.7\text{--}200$ GeV.*

DEBASISH MALLICK (FOR THE STAR COLLABORATION),

National Institute of Science Education and Research, HBNI, Jatni-752050,
INDIA

Received July 30, 2022

1 The production mechanism of deuterons, which have binding energy of
2 2.2 MeV, is a topic of current interest in high energy heavy-ion collisions.
3 Two of common scenarios are statistical thermal process and coalescence of
4 nucleons. Cumulants of deuteron number and proton-deuteron correlations
5 are sensitive to these physics processes. They are also sensitive to the
6 choice of canonical versus grand canonical ensemble in statistical thermal
7 models. We report the first measurements of cumulant ratios (up to 4th
8 order) of the deuteron number and proton-deuteron correlations in Au+Au
9 collisions at $\sqrt{s_{NN}} = 7.7\text{--}200$ GeV. Comparisons of the measurements to
10 the thermal model calculations with a grand canonical, canonical ensemble,
11 and the UrQMD model combined with a coalescence mechanism provide key
12 insights into the mechanism of deuteron production in heavy-ion collisions.

13

1. Introduction

14 One of the primary goals of heavy-ion collision experiments is to study
15 the phases of matter under extreme conditions such as temperature and/or
16 pressure. High-energy heavy-ion collision experiments have established a
17 new state of matter known as Quark-Gluon Plasma (QGP). Studying the
18 particle production mechanism in such collisions gives a direct opportunity
19 to study this state of matter. The mean yields of hadrons as well as of
20 light nuclei produced in central heavy-ion collisions can be explained within
21 the thermal statistical model for suitable choices of chemical freeze-out pa-
22 rameters. The typical values of chemical freeze-out temperature (T) of the
23 system created in such collisions vary around 140 to 155 MeV [1–3]. The
24 puzzle on the light nuclei production in these collisions naturally arises as
25 their binding energies are of the order of only a few MeV, which is much

* Presented at XXIXth International Conference on Ultra-relativistic Nucleus-Nucleus Collisions, April 4-10, 2022, KRAKÓW, POLAND

26 lower than the freeze-out temperature of the medium. The other approach
 27 to understand the production of light nuclei is the coalescence mechanism,
 28 where light nuclei are formed by coalescing protons and neutrons close by
 29 in the phase space. This approach predicts the constituent nucleon num-
 30 ber scaling [4] of the elliptic flow of light nuclei. Such a property has been
 31 observed in the STAR experiment [5].

32 Higher order cumulants have been extensively studied to understand
 33 the thermodynamics of the system. In particular, higher order cumulants
 34 of event-by-event deuteron number distribution and proton-deuteron corre-
 35 lations are predicted to have distinct natures in the thermal and coalescence
 36 models [6]. Further, theoretical calculations suggest that the production of
 37 light nuclei might be affected by the presence of a QCD critical point and
 38 first-order phase transition due to their sensitivity to the local fluctuations
 39 in neutron density [7,8]. As deuterons carry two baryons, their fluctuations
 40 will also enhance our understanding of baryon number fluctuation. In these
 41 proceedings, we report the measurements of cumulant ratios of deuteron
 42 number distribution and proton-deuteron correlation for 0-5% and 70-80%
 43 centralities in Au+Au collisions for $\sqrt{s_{NN}} = 7.7$ to 200 GeV.

44

2. Analysis methods

45 Events of minimum-bias Au+Au collisions at $\sqrt{s_{NN}} = 7.7, 11.5, 14.5,$
 46 $19.6, 27, 39, 54.4, 62.4,$ and 200 GeV are analyzed for the measurement
 47 using the STAR detector at RHIC. Deuterons are identified using both
 48 Time Projection Chamber (TPC) and Time-of-Flight (TOF) detectors in
 49 the transverse momentum (p_T) range of 0.8 to 4 GeV/ c and within mid-
 50 rapidity ($|y| < 0.5$). For proton-deuteron correlation measurement, protons
 51 are identified in $|y| < 0.5$, using only TPC for $0.4 < p_T < 0.8$ GeV/ c ,
 52 while both TPC and TOF detectors are used for the range $0.8 < p_T < 2.0$
 53 GeV/ c [9,10]. The collision centrality is determined from the charged parti-
 54 cle multiplicity (measured within $|\eta| < 1$) excluding the particles of interest
 55 (protons and deuterons) to avoid the auto-correlation effect. To suppress
 56 the effects of volume fluctuations, cumulants are calculated in each multi-
 57 plicity bin and centrality bin-width correction is applied [11]. Cumulants
 58 are also corrected for the finite detection efficiencies and acceptance effects
 59 with the assumption that the detector response is binomial in nature [12].
 60 Statistical uncertainties are calculated using the bootstrap method [10,13].
 61 For the systematic uncertainty estimation, track quality, particle identifi-
 62 cation criteria, and the detection efficiencies are varied within reasonable
 63 ranges.

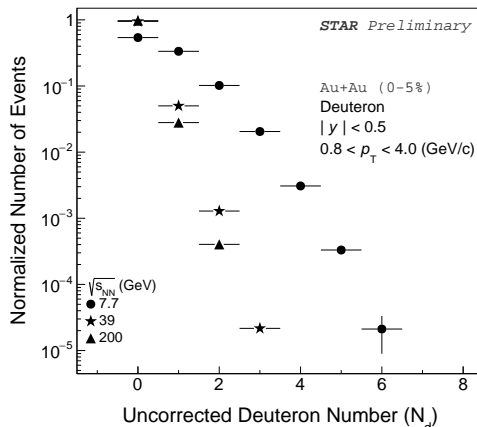


Fig. 1. Event-by-event deuteron number distribution for central (0-5%) Au+Au collisions for $\sqrt{s_{NN}} = 7.7, 39,$ and 200 GeV. Deuteron numbers are not corrected for efficiency.

64

3. Results

65 Figure 1 shows event-by-event deuteron number distribution for central
 66 0-5% Au+Au collisions for $\sqrt{s_{NN}} = 7.7, 39,$ and 200 GeV. Deuteron numbers
 67 shown are un-corrected for the detection efficiency. The mean and width,
 68 as can be seen from the distributions, increase as collision energy decreases.
 69 This trend can be understood from the fact that baryon chemical potential
 70 also increases towards lower $\sqrt{s_{NN}}$, resulting in enhanced production of
 71 deuterons.

72 Cumulants calculated from the deuteron distributions are corrected for
 73 centrality bin-width effect and detection efficiencies. Figure 2 shows the
 74 deuteron $\kappa\sigma^2$, $S\sigma$, σ^2/M , and proton-deuteron correlation for central 0-5%
 75 and peripheral 70-80% Au+Au collisions at $\sqrt{s_{NN}} = 7.7$ to 200 GeV. At
 76 higher $\sqrt{s_{NN}}$, the cumulant ratios in 0-5% centrality are close to the Pois-
 77 son baseline (unity) and deviate from unity as $\sqrt{s_{NN}}$ decreases. In central
 78 collisions they show smooth dependence on collision energy. The $\kappa\sigma^2$ shows
 79 the largest deviation from unity compared to other two ratios which involve
 80 lower order cumulants. Suppression arises because of global baryon number
 81 conservation, which affects the measurements performed at mid-rapidity. In
 82 central collisions at lower $\sqrt{s_{NN}}$, increased baryon stopping and acceptance
 83 covering larger part of phase-space result in more observable effect of baryon
 84 number conservation. Corresponding results in 70-80% peripheral central-
 85 ity show weak dependence on $\sqrt{s_{NN}}$. The calculations for thermal model
 86 with Grand Canonical Ensemble (GCE) and Canonical Ensemble (CE) are

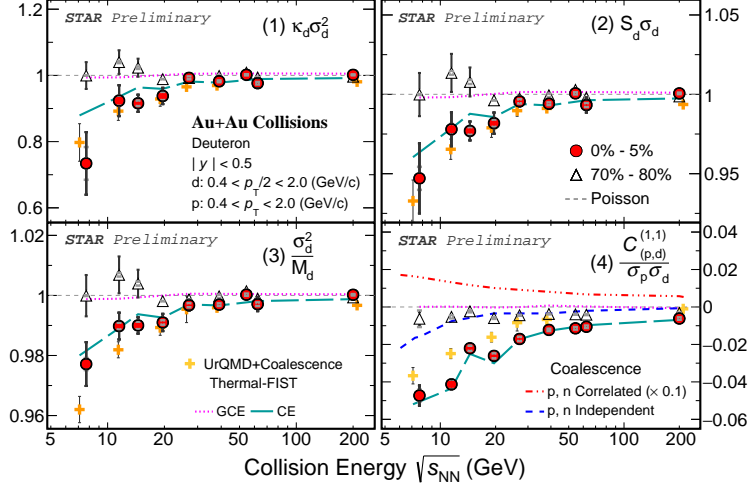


Fig. 2. Cumulant ratios of deuteron distributions and proton-deuteron correlation shown as a function of collision energy. Red circle and open triangle markers represent measurements for most central (0-5%) and peripheral (70-80%) collisions, respectively. Bars and brackets symbols represent the statistical and systematic uncertainties, respectively. UrQMD+phase-space coalescence calculations are shown using orange cross markers. Thermal-FIST model calculations for GCE and CE are shown using magenta and cyan dashed lines, respectively. In panel (4), results for correlated and independent proton (and neutron) distributions in the toy model simulation of coalescence process from Ref. [6] are shown using red and blue dashed lines, respectively.

87 obtained from Thermal-FIST [14]. These calculations are performed for
 88 central 0-5% collisions with experimental acceptances. The chemical freeze-
 89 out parameters published by the STAR experiment [1] from fit of hadronic
 90 mean yields are used for the calculation. The CE Thermal-FIST model uses
 91 a volume called canonical correlation volume, V_c , over which the exact con-
 92 servation of baryon number is implemented. V_c parameter is varied at each
 93 $\sqrt{s_{NN}}$ for a reasonable agreement of model calculations with the measured
 94 cumulant ratios and the Pearson's coefficient. The cyan-colored dashed lines
 95 represent results corresponding to minimum χ^2 obtained from the scan of
 96 parameter V_c to explain the cumulant ratios and proton-deuteron correla-
 97 tion. Measurements favour V_c parameter close to $4dV/dy$ at higher $\sqrt{s_{NN}}$,
 98 which decreases towards lower collision energies. For the condition $V_c \rightarrow \infty$,
 99 the measured part of the system approaches to GCE limit. Smaller values
 100 of V_c at lower collision energies imply the importance of baryon number
 101 conservation effect on the measurements.

102 For higher $\sqrt{s_{NN}}$, cumulant ratios in central 0-5% show reasonable agree-
 103 ment with both GCE and CE thermal model expectations. However, GCE
 104 seems to fail to describe the ratios for $\sqrt{s_{NN}} \leq 20$ GeV. The CE thermal
 105 model predicts the suppression of cumulant ratios. The corresponding re-
 106 sults for 0-5% Au+Au collisions from a UrQMD model, combined with a
 107 phase-space coalescence mechanism (with a hard cut on relative momentum
 108 and distance between protons and neutrons), also predict energy dependence
 109 trend of cumulant ratios.

110 Panel (4) of the Fig. 2 shows that for all collision energies and cen-
 111 tralities presented the Pearson correlation coefficient between proton and
 112 deuteron number is negative. This anti-correlation becomes stronger for
 113 central collisions as $\sqrt{s_{NN}}$ decreases. Corresponding results for peripheral
 114 collisions do not show any $\sqrt{s_{NN}}$ dependence and are close to zero. GCE
 115 thermal model fails to predict the anti-correlation. The CE thermal model
 116 correctly predicts the sign and $\sqrt{s_{NN}}$ dependence trend of the correlation.
 117 Results from the simple statistical simulation of coalescence process from
 118 Ref. [6] are shown for central collisions for two assumptions on the proton
 119 and neutron number distributions. In one case, they are fully correlated
 120 (*i.e.* $N_p = N_n$, where N_p and N_n are proton and neutron numbers in one
 121 event, respectively) and in the other case they are completely independent.
 122 Neither correlated nor independent assumption for proton and neutron num-
 123 ber reproduce the data. However, UrQMD+coalescence model predicts the
 124 trend of the experimental data in central 0-5% collisions. This suggests that
 125 the phase-space density information of constituent nucleons is important
 126 for the coalescence mechanism. The negative sign of the Pearson correla-
 127 tion coefficient suggests the importance of baryon number conservation in
 128 hadron-nuclei correlations.

129 4. Summary

130 We presented the cumulant ratios of deuteron number and proton-deuteron
 131 correlations for central 0-5% and peripheral 70-80% Au+Au collisions at
 132 $\sqrt{s_{NN}} = 7.7$ to 200 GeV. Cumulant ratios at higher $\sqrt{s_{NN}}$ are close to Pois-
 133 son baseline, unity, and are suppressed as the collision energy decreases. The
 134 GCE thermal model fails to describe the cumulant ratios below $\sqrt{s_{NN}} = 20$
 135 GeV. Canonical ensemble thermal model and the UrQMD model combined
 136 with a coalescence mechanism, both of which have the baryon number con-
 137 servation implemented, correctly predict the suppression. We also observe
 138 that Pearson correlation coefficient between proton and deuteron numbers is
 139 negative for all collision energies and centralities presented, which becomes
 140 even more negative for central 0-5% collisions as $\sqrt{s_{NN}}$ decreases. The GCE
 141 model fails to predict the sign of this correlation. However, both the CE

142 thermal model and UrQMD+coalescence model correctly predict the sign
143 and energy dependence trend of the experimental measurement.

144

5. Acknowledgments

145 We acknowledge the financial support by Department of Atomic Energy,
146 Govt. of India.

References

- 147 [1] L. Adamczyk *et al.* [STAR], Phys. Rev. C **96** (2017) no.4, 044904
148 doi:10.1103/PhysRevC.96.044904
- 149 [2] A. Andronic, P. Braun-Munzinger, K. Redlich and J. Stachel, Nature **561**
150 (2018) no.7723, 321-330 doi:10.1038/s41586-018-0491-6
- 151 [3] J. Adam *et al.* [STAR], Phys. Rev. C **99** (2019) no.6, 064905
152 doi:10.1103/PhysRevC.99.064905
- 153 [4] T. Z. Yan *et al.* Phys. Lett. B **638** (2006), 50-54
154 doi:10.1016/j.physletb.2006.05.018
- 155 [5] L. Adamczyk *et al.* [STAR], Phys. Rev. C **94** (2016) no.3, 034908
156 doi:10.1103/PhysRevC.94.034908
- 157 [6] Z. Fecková, J. Steinheimer, B. Tomášik and M. Bleicher, Phys. Rev. C **93**
158 (2016) no.5, 054906 doi:10.1103/PhysRevC.93.054906
- 159 [7] K. J. Sun, L. W. Chen, C. M. Ko and Z. Xu, Phys. Lett. B **774** (2017), 103-107
160 doi:10.1016/j.physletb.2017.09.056
- 161 [8] E. Shuryak and J. M. Torres-Rincon, Phys. Rev. C **100** (2019) no.2, 024903
162 doi:10.1103/PhysRevC.100.024903
- 163 [9] J. Adam *et al.* [STAR], Phys. Rev. Lett. **126** (2021) no.9, 092301
164 doi:10.1103/PhysRevLett.126.092301
- 165 [10] M. Abdallah *et al.* [STAR], Phys. Rev. C **104** (2021) no.2, 024902
166 doi:10.1103/PhysRevC.104.024902
- 167 [11] X. Luo, J. Xu, B. Mohanty and N. Xu, J. Phys. G **40** (2013), 105104
168 doi:10.1088/0954-3899/40/10/105104
- 169 [12] T. Nonaka, M. Kitazawa and S. Esumi, Phys. Rev. C **95** (2017)
170 no.6, 064912 [erratum: Phys. Rev. C **103** (2021) no.2, 029901]
171 doi:10.1103/PhysRevC.95.064912
- 172 [13] A. Pandav, D. Mallick and B. Mohanty, Nucl. Phys. A **991** (2019), 121608
173 doi:10.1016/j.nuclphysa.2019.08.002
- 174 [14] V. Vovchenko and H. Stoecker, Comput. Phys. Commun. **244** (2019), 295-310
175 doi:10.1016/j.cpc.2019.06.024